Development 127, 2063-2073 (2000)
Printed in Great Britain © The Company of Biologists Limited 2000
DEV2521

OOC-3, a novel putative transmembrane protein required for establishment of cortical domains and spindle orientation in the P_1 blastomere of *C. elegans* embryos

Silke Pichler[1,2], Pierre Gönczy[1,2], Heinke Schnabel[3], Andrei Pozniakowski[1], Anthony Ashford[1], Ralf Schnabel[3] and Anthony A. Hyman[1,2,*]

[1]Max Planck Institute for Cell Biology and Genetics, D-01307 Dresden, Germany
[2]EMBL, Meyerhofstrasse 1, D-69117 Heidelberg Germany
[3]Institut für Genetik, TU Braunschweig, Spielmannstrasse 7, D-38023 Braunschweig, Germany
*Author for correspondence at address 2 (e-mail: hyman@embl-heidelberg.de)

Accepted 14 February; published on WWW 18 April 2000

SUMMARY

Asymmetric cell divisions require the establishment of an axis of polarity, which is subsequently communicated to downstream events. During the asymmetric cell division of the P_1 blastomere in *C. elegans*, establishment of polarity depends on the establishment of anterior and posterior cortical domains, defined by the localization of the PAR proteins, followed by the orientation of the mitotic spindle along the previously established axis of polarity. To identify genes required for these events, we have screened a collection of maternal-effect lethal mutations on chromosome II of *C. elegans*. We have identified a mutation in one gene, *ooc-3*, with mis-oriented division axes at the two-cell stage. Here we describe the phenotypic and molecular characterization of *ooc-3*. *ooc-3* is required for the correct localization of PAR-2 and PAR-3 cortical domains after the first cell division. OOC-3 is a novel putative transmembrane protein, which localizes to a reticular membrane compartment, probably the endoplasmic reticulum, that spans the whole cytoplasm and is enriched on the nuclear envelope and cell-cell boundaries. Our results show that *ooc-3* is required to form the cortical domains essential for polarity after cell division.

Key words: Polarity, Spindle orientation, *ooc-3*, Cortical domain, Endoplasmic reticulum, PAR protein, Asymmetric division, *C. elegans*

INTRODUCTION

The generation of cell diversity depends, among other mechanisms, on asymmetric cell divisions (Horvitz and Herskowitz, 1992). For cells to divide asymmetrically, they must first determine an axis of polarity and then communicate this polarity to downstream targets, such as the cytoskeleton (Gönczy and Hyman, 1996). Recent work has suggested that an early event in the establishment of cell polarity is the formation of cortical domains, regions of the cell cortex containing specialized sets of proteins. In the yeast *S. cerevisiae*, growth of the bud from the mother is accompanied by formation of cortical domains at the growing bud tip (Madden and Snyder, 1998). *Drosophila* neuroblasts form an apical basolateral axis in which the apical and basolateral surfaces represent different cortical domains (Kuchinke et al., 1998). In *C. elegans* embryos, establishment of the axis of polarity is accompanied by formation of two cortical domains represented by the PAR proteins (Rose and Kemphues, 1998).

The correct delivery of membrane proteins into cortical domains is essential for polarization and this targeting may already occur in the endoplasmic reticulum (ER). For example, in *S. cerevisiae*, Axl2, a transmembrane protein required for bud site selection, is transported to nascent bud tips by a mechanism that requires Erv14, a protein that localizes to the ER (Powers and Barlowe, 1998). In erv14 mutants, Axl2 accumulates in the ER and this correlates with a defect in bud site selection (Powers and Barlowe, 1998). Interestingly, erv14 is homologous to the *cornichon* gene in *Drosophila*, which is required for polarity of egg chambers during oogenesis (Roth et al., 1995). Therefore specific targeting of transmembrane proteins during their passage through the ER is important for the establishment of polarity in several systems, but these issues remain understudied.

The early embryonic cleavages of the nematode *C. elegans* provide an excellent system to study the establishment of polarity because defined cortical domains are established soon after fertilization, and these cortical domains trigger downstream events that are easy to follow by microscopy. In the cells of the P-lineage the cortical domains are established via the localization of PAR-3, PAR-6 and PKC-γ at the anterior, and PAR-2 and PAR-1 at the posterior cortices, respectively

(Levitan et al., 1994; Etemad-Moghadam et al., 1995; Guo and Kemphues, 1995; Boyd et al., 1996; Watts et al., 1996; Tabuse et al., 1998). It is thought that PAR-3 first establishes an anterior cortical domain, PAR-2 and PAR-3 then interact, leading to a mutually exclusive distribution, with PAR-3 restricted to the anterior and PAR-2 to the posterior (Rose and Kemphues, 1998). Subsequently this polarity is communicated to downstream events. One set of events is the segregation of cell fate determinants of differentiation, such as P-granules, to one end of the cell prior to division (Strome and Wood, 1983). In a second set of events, the axis of polarity is communicated to the cytoskeleton, triggering a 90º rotation of the centrosome-nucleus complex, aligning the spindle along the antero-posterior axis (Albertson, 1984; Hyman, 1989).

We know very little about the cues that establish these cortical domains or how they are communicated to the cytoskeleton. In the zygote P_0, the cue for the establishment of the anterior and posterior cortical domains is provided extrinsically by a sperm component that marks the future posterior pole (Goldstein and Hird, 1996). However, similar cortical domains are set up in subsequent cleavages of the P-lineage, and in these divisions the cues that establish these cortical domains are completely unclear.

MATERIALS AND METHODS

Culture conditions and strains

Culture, handling and crossing were as described (Brenner, 1974). The following genes and alleles were used in this study: *mnC1 II dpy-10(e128) unc-52(e444) II/dpy-2(e8) II him-3 (e1147) IV* (Herman, 1978), *mnDf87 II*, *mnDf88 II*, *mnDf89 II* and *mnDf90 II* (Sigurdson et al., 1984), *ooc-1(mn250)*, *ooc-3(mn241)*, *mel-8(b312)*, *mel-9(b293ts)*, *mel-11(it26)*, *mel-13(b306)*, *mel-15(it38)*, *mel-18(b300)*, *mel-19(b310)*, *mel-21(it9)*, *mel-22(it30)* (Kemphues et al., 1988).

Isolation and genetic analysis of *t1308*

L4-stage hermaphrodites of genotype *mnC1 II/dpy-2(e8) II; him-3(e1147) IV* were mutagenized using 50 mM ethyl methane sulfonate for 4 hours according to standard procedures (Brenner, 1974). Mutagenized *mnC1/dpy-2; him-3* F1 L4 hermaphrodites were grown individually for 3 days on agar plates at 25°C. The plates were scored for the presence of *dpy-2* progeny. Dumpy L4 or young adult hermaphrodites of each plate were transferred to a new plate and incubated at 25°C. The mutants were mapped with the deficiencies *mnDf88* and *mnDf89* (R. Schnabel, H. Schnabel and R. Feichtinger, unpublished). From 13700 mutagenized genomes, one mutation, *t1308*, failed to rotate the centrosome-nucleus complex in 100% of embryos. *ooc-3* has previouslybeen placed under *mnDf83 II*, *mnDf87 II*, *mnDf89 II* and *mnDf90* (Sigurdson et al., 1984). Our deficiency mapping put *t1308* under *mnDf89*. *ooc-3(mn241)* and *mel-19(b310)* failed to complement *t1308*.

Germline transformation and RNA interference (RNAi) analysis

Heterozygous *ooc-3(mn241) unc-4(e120)/mnC1 dpy-10(e128) unc-52(e444) II*, were injected with a mixture of the DNA (5 ng/µl) to be tested and *rol-6* DNA (100 ng/µl) (Mello et al., 1991). Roller homozygous *ooc-3* F1 hermaphrodites were placed on separate plates and scored for maternal-effect lethality. The mutation *ooc-3(mn241)* causes 100% lethality in embryos from homozygous hermaphrodites at 25°C. Cosmids B0334, C05D12 and W02B12 were injected. Only B0334 gave rescue. To define the *ooc-3* locus, the ends of the overlapping cosmids C51D6, T18C10, F46F12 and C56C6 were sequenced. The end positions are as follows: 27791 (on W02B12)-38918 (on B0334) for C51D6, 28608 (on W02B12)-35255 (on B0334) for T18C10, 17816 (on W02B12)-22627 (on B0334) for F46F12 and C56C6 (on W02B12)-11585 (on B0334) for C56C6. The positions of the PCR fragments on the rescuing cosmid B0334 are as follows: 37-8506 for Bcl1, 7521-15966 for Bcl2, 14946-22099 for Bcl3, 10061-17801 for Bcl4 and 13741-16902 for B11.

RNAi was performed with modifications of Fire et al. (1998). The region 14192-16143 on B0334 was amplified from cosmid B0334 using standard PCR procedures. To interfere with the expression of PAR-3 in wild-type and *ooc-3* mutant worms, plasmid P5A (Etemad-Moghdam et al., 1995) was linearized with *Bam*HI and subsequently used as template for transcription reactions.

Sequencing of mutant alleles and cDNAs

The fragment B11 (from bases 13741 to 16902 on B0334) was amplified from wild-type and *ooc-3(t1308)* and *ooc-3(mn241)* homozygous mutant worms using whole-worm PCR. 50 worms were transferred to a PCR tube containing 10 µl lysis buffer (10 mM Tris, pH 8.3, 50 mM KCl, 2.5 mM $MgCl_2$, 0.45% Tween-20, 0.005% gelatine) and 60 µg/ml proteinase K. Worms were frozen in liquid nitrogen for 10 minutes and incubated for 60 minutes at 60°C and 15 minutes at 95°C. The available cDNAs (yk383, yk524, yk588, yk589, yk645, yk332) were sequenced. None of these cDNAs is complete, but yk383 misses only the two very 5′ codons of the predicted B0334.11.

Antibodies and immunofluorescence

PAR-2 antibodies: a 741 bp fragment starting at nucleotide 943 in the *par-2* ORF was cloned into pGEX-4T-3 (Pharmacia). The GST fusion protein was purified, injected into rabbits and purified according to standard procedures. A single band of the expected molecular mass was obtained by western blot (data not shown). PAR-3 antibodies: a 750 bp fragment starting at nucleotide 2053 in the *par-3* ORF was cloned into pGEX-4T-3 (Pharmacia). ZYG-9; antibodies were raised against a C-terminal peptide of ZYG-9, and will be described elsewhere. OOC-3 antibodies (OOC3Ct2): a C-terminal peptide was synthesized (amino acids 432-448). For affinity purification, the crude antisera were passed over a column containing the coupled peptide. Bound antibodies were eluted with 100 mM glycine, pH 1.9, and dialyzed against PBS. OOC-3 antibody was used at 1:500 PBS.

Staining of microtubules, ZYG-9, P-granules, PAR-2 and PAR-3 by indirect immunofluorescence was performed with modifications of standard procedures (Gönczy et al., 1999). To stain for OOC-3, embryos were fixed in 75% methanol, 3.7% formaldehyde and 0.5× PBS for 15 minutes at –20°C and subsequently for 15 minutes in –20°C methanol. After rehydration in PBS for 10 minutes, embryos were incubated for 1 hour with 30 µl of primary antibody. Peptide competition was performed in which the OOC-3 antibody was pre-incubated with 0.1 mg/ml peptide for 15 minutes. Actin staining was as described in Waddle et al. (1994).

RESULTS

ooc-3 is required for proper spindle orientation in the P_1 blastomere of two-cell stage *C. elegans* embryos

We wanted to identify genes required for the establishment of polarity and spindle orientation. The most obvious manifestation of polarity is the orientation of the cleavage axes, which in the P-lineage is mediated by a 90° rotation of the centrosome-nucleus complex (Fig. 1). Therefore we screened a collection of recessive maternal-effect lethal mutations on linkage group II by time-lapse DIC

videomicroscopy for strains defective in P_1 rotation (see Materials and Methods). In one strain, *t1308*, rotation of the centrosome-nucleus complex failed in 100% of embryos examined (Fig. 2b). Complementation analysis revealed that *t1308* is allelic to *ooc-3(mn241)* (Sigurdson et al., 1984) and *mel-19(b310)* (Kemphues et al., 1988) (Table 1). From now on 'ooc-3 mutant embryos' (in text and Fig. legends) means 'ooc-3(tl308) mutant embryos'. Besides the fully penetrant defect in P_1 rotation, *ooc-3* mutant embryos showed various additional and non-penetrant abnormalities in the first two-cell stages. These include defects in meiotic and mitotic chromosome segregation, rotation of the centrosome-nucleus complex in P_0, posterior displacement of the spindle during anaphase in P_0 and the correlation of the AB and P_1 cell cycle times (Table 1).

A striking feature of *ooc-3* mutant embryos was their reduced embryo size (Table 1, Fig. 2b). To test whether the defect in P_1 rotation in *ooc-3* mutant embryos was a consequence of steric inhibition caused by small embryo size, we investigated whether P_1 rotation could occur in other mutant strains that give rise to small embryos. We found that in embryos of two such mutant strains, *t1453* and *t1655* (Gönczy et al., 1999), P_1 rotation was not inhibited, suggesting that the defect in P_1 rotation observed in *ooc-3* mutant embryos is not a consequence of reduced embryo size.

The centrosome-centrosome distance is defective in *ooc-3* mutant embryos

In wild-type embryos, P_1 rotation is thought to depend on the attachment of astral microtubules emanating from one centrosome to a site at the anterior cortex enriched in actin (Hyman and White, 1987; Hyman, 1989; Waddle et al., 1994; Skop and White, 1998) (see Fig. 1). Tubulin staining revealed that microtubules in *ooc-3* mutant embryos were indistinguishable from wild type; astral microtubules were numerous and long enough to reach the cortex (data not shown). However, tubulin staining indicated that the angle between the two centrosomes during prophase, the time at which P_1 rotation occurs in wild type (Hyman, 1989) was altered in some *ooc-3* mutant embryos (data not shown).

To investigate this observation further, we stained fixed wild-type and *ooc-3* mutant embryos with an antibody against a centrosomal marker, ZYG-9 (Matthews et al., 1998). As expected, in wild type the two centrosomes were at opposite sides of the nucleus, subtending an angle of about 180° with respect to the center of the nucleus. The whole centrosomal-

Table 1. Summary of DIC phenotypes of the three *ooc-3* alleles, the transheterozygous combinations and transheterozygotes of *ooc-3* and deficiencies uncovering the *ooc-3* region

Genotype	Temperature (°C)	Size (μm)	Meiotic defect (%)[a]	P_0 rotation defect (%)[b]	Cleavage furrow position (% egg length)[c]	Chromosome segregation defect (%)[d]	P_1 rotation defect (%)[e]	P_1 timing defect (%)[f]	Mel[h]
Wild type	25	49.5±1.7	0 (20)[i]	5 (20)	56.2±2.2	0 (20)	0 (19)	0/0 (11)	0 (20)
t1308	25	31.2±4.7	63 (11	10 (11)	54.2±2.8	27 (11)	100 (11)	10/64 (11)	100 (80)
t1308 wt	25	49.4±2.1	0 (10)	0 (10)	55.8±1.8	0 (10)	0 (10)	0/10 (10)	0 (20)
mn241	25	33.8±3.0	25 (20)	45 (20)	52.6±2.5	35 (20)	80 (20)	15/40 (20)	100 (80)
b310	25	39.5±7.0	17 (12)	8 (12)	56.1±2.7	33 (12)	92 (12)	17/67 (12)	95 (39)[j]
t1308 mn241	25	32.5±5.4	64 (11)	73 (11)	-	40 (10)	100 (10)	40/10 (10)	100 (17)
t1308 b310	25	50.1±2.7	0 (12)	10 (11)	-	18 (17)	68 (13)	89 (19)	97 (37)[k]
ooc-3 (t1308) mnDf87	25	31.22±6.6	0 (3)	80 (10)	52.7±3.5	25 (16)	94 (16)	14/29 (14)	100 (28)
ooc-3(t1308) mnDf90	25	28.4±3.0	0 (1)	100 (7)	-	0 (11)	100 (10)	20/30 (10)	100 (10)
ooc-3 (b310) mnDf87	25	34.2±3.6	30 (9)	75 (12)	52.3±2.1	40 (15)	100 (14)	36/50 (14)[g]	100 (74)

[a]After fertilization, one female and one male pronucleus form in wild-type embryos. Meiotic defects are revealed by aberrant numbers of female pronuclei (O'Connell et al., 1998; Gönczy et al., 1999).

[b]In one-cell stage wild-type embryos the centrosome-nucleus complex undergoes a 90° rotation (P_0 rotation), which orients the mitotic spindle along the longitudinal axis of the embryo. In embryos defective for P_0 rotation the centrosome-nucleus complex does not rotate, the spindle sets up transverse to the longitudinal axis of the embryo and, subsequently, a 90° rotation of the spindle occurs ('spindle rescue') (O'Connell et al., 1998; Gönczy et al., 1999). Partial rotation and aberrant rotation movements are not considered in this table.

[c]In P_0 the mitotic spindle assembles in the cell center but subsequently in anaphase gets displaced towards the posterior pole. To investigate anaphase displacement, we measured the position of the cleavage furrow which ingresses equidistant from the spindle poles. Whereas in wild-type embryos cleavage furrow ingression occurs at 56% egg length in average, it occurs more symmetrically in *ooc-3* mutant embryos.

[d]Chromosome segregation defects are revealed by the appearance of karyomeres after the reformation of nuclei in AB and P_1 (O'Connell et al., 1998; Gönczy et al., 1999).

[e]In P_1 the centrosome-nucleus complex rotates 90° and subsequently the spindle sets up along the longitudinal axis of the embryo (Hyman and White, 1987). In embryos defective for P_1 rotation the centrosome-nucleus complex does not rotate and the spindle sets up transverse to the longitudinal axis of the embryo .

[f]In wild-type embryos nuclear envelope breakdown (NEB) in AB occurs about 2 minutes ahead of P_1 (Hyman and White, 1987). The P_1 cell cycle timing is defective when the delay between AB and P_1 NEB is less than 1 minute or more than 3 minutes. Values are given as x/y; x indicates the percentage of embryos in which the P_1 cell cycle is accelerated and y reveals the percentage of embryos in which the P_1 cell cycle is slowed down.

[g]In all the cases in which the P_1 cell cycle was accelerated (in two of the four cases P_1 even divides before AB), there is no rotation in P_0 and the spindle appeared to sweep around the whole cytoplasm (or even the whole embryo in the eggshell) during spindle rescue. The acceleration in the P_1 cell cycle in these embryos is therefore most probably a secondary effect caused by the failure of P_0 rotation. Embryos in which P_0 rotation occurred correctly but the P_1 cell cycle was accelerated were never observed.

[h]Mel, maternal-effect lethality; one wild-type worm gives rise to about 200 hatching embryos. We define the mutation as maternal-effect lethal (100%) if less than 10 embryos/worm hatch.

[i]Throughout the table, the numbers in parentheses are the numbers of embryos (for the Mel test, the number of worms) analysed.

[j]3% of worms gave rise to about 20 hatching embryos. 2% gave rise to 50 and 2% to 100 hatching embryos.

[k]3% of worms gave rise to 200 hatching embryos.

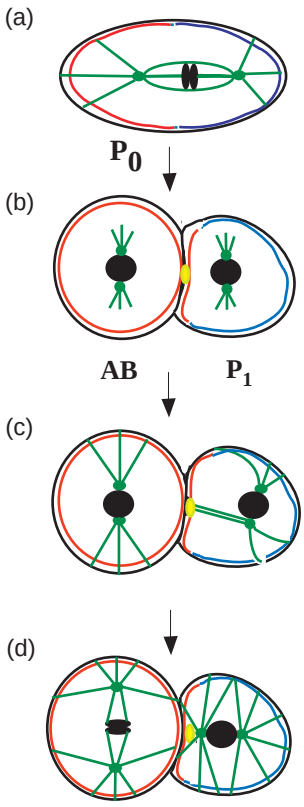

Fig. 1. A 90° rotation of the centrosome-nucleus complex in P_1 aligns the mitotic spindle along the antero-posterior axis of the embryo. (a) P_0 at anaphase spindle positioning. PAR-2 (blue) and PAR-3 (red) are proteins whose polarized localization is required for the establishment of the antero-posterior in P_0 and subsequently in P_1. After rotation of the centrosome-nucleus complex, the spindle sets up in the cell center and subsequently gets displaced towards the posterior. (b) After duplication and migration of the centrosomes in AB and P_1, both the AB and the P_1 centrosome pairs are aligned transverse to the antero-posterior axis of the embryo. (c,d) In P_1, the centrosome-nucleus complex subsequently undergoes a 90° rotation (P_1 rotation), which aligns it along the antero-posterior axis. P_1 rotation depends on the establishment of the antero-posterior axis by localization of PAR-2 and PAR-3 to opposing cortical domains and the subsequent communication of that polarity to the cytoskeleton. The physical process of P_1 rotation is thought to be mediated as follows: astral microtubules (in green) emanating from one of the two centrosomes (green circle) attach at a site at the anterior cortex (yellow ellipse) enriched in actin, the actin capping proteins and components of the dynactin complex. Subsequent shortening of astral microtubules places this centrosome next to the anterior cortical site, which leads to a 90° rotation of the centrosome-nucleus complex. Anterior is to the left and posterior to the right.

nuclear complex then rotates by 90°, while keeping the angle between the centrosomes at 180° (*n*=10) (Fig. 3b). However, in *ooc-3* mutants, the subtended angle was reduced to less than 120° in 40-54% of *ooc-3* mutant embryos (*t1308*: 40%, *n*=10; *mn241*: 54%, *n*=11; *b310*: 50%, *n*=10 (Fig. 3c). This resulted in both centrosomes being positioned nearer to the anterior cortex than in wild type. One plausible explanation for the abnormal centrosome position is that pulling forces are exerted equally on both centrosomes.

The anterior cortical site is defective in *ooc-3* mutant embryos

We next examined the enrichment of actin at the anterior cortical site, which is known to be required for P_1 rotation in wild-type. In all 21 wild-type embryos examined, the cortical site formed a discrete ring-like structure either symmetrically or slightly asymmetrically positioned (Fig. 4a,b). In contrast, in *ooc-3* mutant embryos the cortical site was no longer restricted to a defined location in 78% of the embryos examined (*n*=18). Either the cortical site was clearly enlarged (Fig. 4c,d), or several ring- or dot-like structures were observed (Fig. 4e,f). Thus, *ooc-3* appears to be required for the restriction of actin to the defined ring-like structure at the anterior cortex, which is thought to represent the microtubule attachment site. It is possible that this expanded site allows capture of microtubules from both centrosomes, preventing rotation of the centrosome-nucleus complex, thus pulling them both around the nucleus towards the anterior cortex.

P-granule distribution is affected in the P_1 blastomere of *ooc-3* mutant embryos

The defects in the structure and the size of the anterior cortical site and the position of the centrosomes in *ooc-3* mutant embryos might be due to a primary defect in the organization of the cytoskeleton. Alternatively, *ooc-3* might be required to re-establish an axis of polarity from which the defects in the cytoskeleton are a secondary consequence. To distinguish between these two possibilities, we examined the distribution of P-granules, which are polarity markers segregated exclusively to P_1 during the first cell division and localize to the posterior pole of P_1 in prophase (Strome and Wood, 1983). We found that P-granules were properly segregated to P_1 during the first cell division in all *ooc-3* mutant embryos

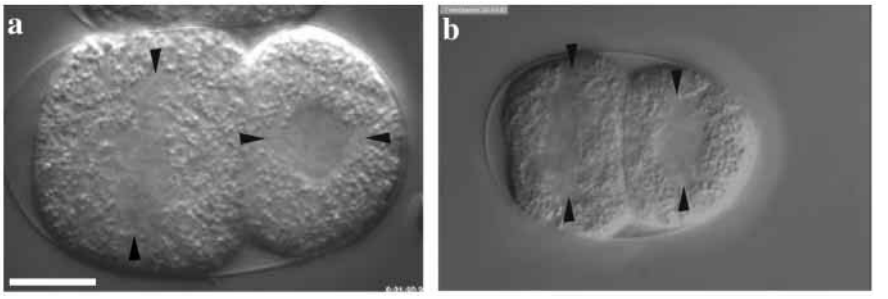

Fig. 2. Rotation of the centrosome-nucleus complex is defective in *ooc-3* mutant embryos. P_1 rotation does not take place in *t1308* mutant embryos. Arrowheads point to the centrosomes. Anterior is to the left and posterior to the right. Both panels are at the same magnification. (a) In two-cell stage wild-type embryos the centrosome pair in P_1 is oriented perpendicular to the one in AB in which the mitotic spindle has already been assembled. Thus, the centrosome-nucleus complex in P_1 is aligned along the antero-posterior axis of the embryo (see Fig. 1). (b) In *t1308* mutant embryos the centrosome-nucleus complex has not rotated in P_1 at the time of spindle assembly in AB (and nor does it thereafter; data not shown). Thus, the centrosome pair in P_1 is aligned transverse to the antero-posterior axis of the embryo. Bar, 10 μm.

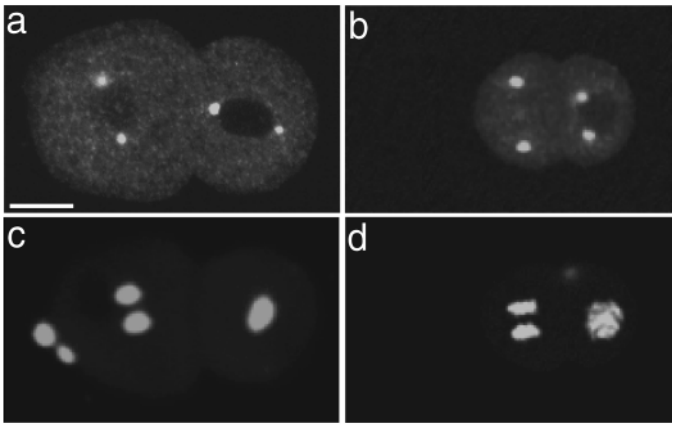

Fig. 3. Centrosome positioning is affected in P_1 of *ooc-3* mutant embryos. Wild type and *ooc-3* mutant embryos were stained with anti-ZYG-9 antibodies and counterstained with Hoechst 33258 to reveal DNA. Images are 2 μm confocal slices. Anterior is to the left. (a,c) Wild-type ZYG-9 marks the centrosomes in both AB and P_1. The centrosome pair in P_1 has almost completed rotation and the angle between the two centrosomes is about 180° (like in AB). P_1 is in prophase. (a) ZYG-9, (c) DNA. (b,d) *ooc-3* mutant ZYG-9 marks the centrosomes in both AB and P_1. The centrosome pairs in AB and P_1 are parallel to each other, which reveals that the centrosome pair in P_1 failed to rotate. In AB the angle between the two centrosomes is about 180° whereas in P_1 the angle is reduced to less than 180°. P_1 is in prophase. (b) ZYG-9, (d) DNA. Bar, 10 μm.

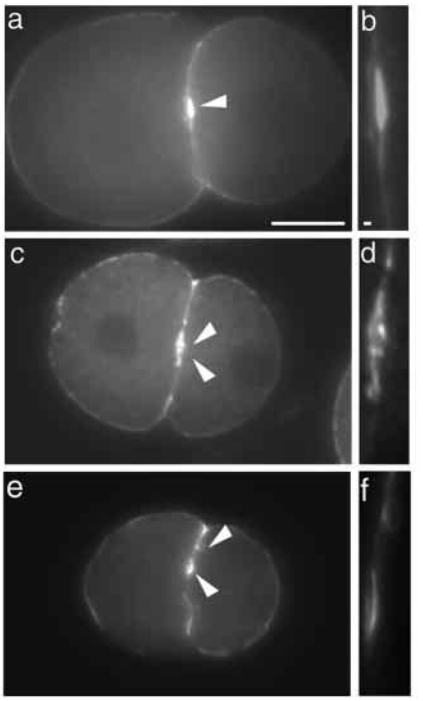

Fig. 4. The organization of the actin cytoskeleton is affected in *ooc-3* mutant embryos. Embryos are stained with an antibody to actin. (a) Wild type, (b) inset of a, (c) *ooc-3* mutant embryo with enlarged anterior cortical site, (d) inset of c, (e) *ooc-3*, (f) inset of e. Bars, 10 μm (a), 0.2 μm (b).

(*mn241*: *n*=12; *t1308*: *n*=6; *b310*: *n*=27; data not shown). However, P-granule distribution was aberrant in P_1. Whereas in wild type P-granules localize to a defined crescent at the posterior cortex of P_1 (*n*=28) (Fig. 5a), this crescent was not restricted to the posterior pole in 20-63% of *ooc-3* mutant embryos (*t1308*: 20%, *n*=10; *mn241*: 60%, *n*=10; *b310*: 56%, *n*=16) (Fig. 5c).

ooc-3 is required to set up the PAR-2 and PAR-3 cortical domains in P_1

To test whether the defects in P-granule segregation and spindle orientation were a consequence of a defect in the establishment of the polarity in P_1 in *ooc-3* mutant embryos, we analyzed the distribution of PAR-2 and PAR-3, which mark the posterior and anterior cortical domains respectively, by immunofluorescence (Rose and Kemphues, 1998). In all wild-type embryos (*n*=32) PAR-2 was localized to the posterior cortex of P_1 (Fig. 6Aa). In contrast, in *ooc-3* mutants PAR-2 was localized at the anterior cortex in 12-75% of the embryos (*t1308*: 12%, *n*=24; *mn241*: 75%, *n*=32; *b310:* 19%, *n*=11; Fig. 6Ac). This suggests that *ooc-3* mutant embryos fail to establish the posterior cortical domain in P_1. PAR-2, however, was properly localized in P_0 in all *ooc-3* mutant alleles (*mn241*: *n*=40; *t1308*: *n*=9; *b310*: *n*=31; data not shown). Similar to wild-type, PAR-2 was absent in the anterior blastomere AB of all two-cell stage *ooc-3* mutant embryos examined (*mn241*: *n*=40; *t1308*: *n*=9; *b310*: *n*=31; Fig. 6Ac). Thus, the cortical localization of PAR-2 is specifically affected in the P_1 blastomere of *ooc-3* mutant embryos.

We also found that PAR-3 localization was affected in *ooc-3* mutant embryos. Whereas in all wild-type embryos PAR-3 was restricted to the anterior cortex of P1 (*n*=14) (Fig. 6Ba), PAR-3 was evenly distributed around the cortex of P_1 in 32-83% of *ooc-3* mutant embryos (*t1308*: 53%, *n*=13; *mn241*: 83%, *n*=38; *b310*: 32%, *n*=25; Fig. 6Bc). In contrast, PAR-3 was properly restricted to the anterior cortical domain in P_0 in all embryos of *mn241* (*n*=29) and *b310* (*n*=43) and in almost all embryos of *t1308* (18% uniformly around the cortex, *n*=17; data not shown). Furthermore, PAR-3 was correctly distributed throughout the cortex in AB (*t1308*: *n*=13; *mn241*: *n*=38; *b310*: *n*=25) (Fig. 6Bc). Taken together, the mislocalization of PAR-2 and PAR-3 in *ooc-3* mutants suggests that *ooc-3* is required to restrict PAR-2 and PAR-3 to their respective cortical domains in P_1.

ooc-3 is required to restrict PAR-3 to the anterior cortex of the P_1 blastomere

In wild-type embryos the localizations of PAR-2 and PAR-3 are mutually exclusive (Etemad-Moghadam et al., 1995; Boyd et al., 1996). In *par-2* mutants, PAR-3 expands to fill the PAR-2 cortical domain, while in *par-3* mutants, PAR-2 expands to fill the PAR-3 cortical domain. Therefore, *ooc-3* could be required for the localization of PAR-2 to the posterior cortex of P_1, which in turn would restrict PAR-3 to the anterior cortex. Alternatively, *ooc-3* could be required for the localization of PAR-3 to the anterior cortex of P_1, which in turn would restrict PAR-2 to the posterior cortex. To distinguish these possibilities, we asked whether PAR-2 mislocalization in *ooc-3* mutant embryos required *par-3* function. To this end, we examined PAR-2 distribution in *ooc-3* mutant embryos in which expression of *par-3* was silenced with RNAi. We found that silencing of *par-3* expression in *ooc-3* mutant embryos

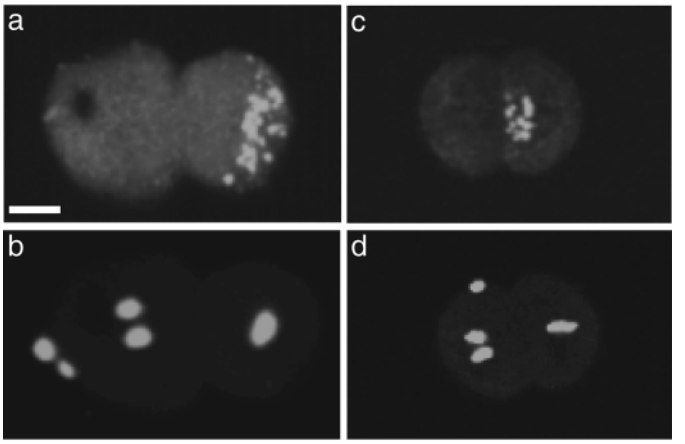

Fig. 5. P-granule localization is affected in two-cell stage *ooc-3* mutant embryos. Wild-type and *ooc-3* mutant embryos were stained with anti-P-granule antibody and counterstained with Hoechst 33258 to reveal DNA. Images are 2 μm confocal slices; in some cases the stage was refocused slightly between channels. All panels are at the same magnification. Anterior is to the left. (a,b) Wild type P-granules are localized as a defined crescent at the posterior cortex of P_1. P_1 is in metaphase. (a) P granules, (b) DNA. (c,d) *ooc-3* mutant (c) P-granules are localized as a defined crescent at the anterior cortex of P_1. (d) DNA. P_1 is in metaphase. Bar, 10 μm.

allowed PAR-2 to localize evenly around the cortex in P_1 in 100% of the embryos (*n*=10) (Fig. 6C). This result demonstrates that PAR-2 is restricted to the anterior cortex in an *ooc-3* mutant because of PAR-3 mislocalization. Moreover, this result suggests that *ooc-3* function is normally required to restrict PAR-3 to the anterior cortex of P_1, which in turn restricts PAR-2 to the posterior cortex.

The mislocalization of PAR-3 partially inhibits P_1 rotation in *ooc-3* mutant embryos

In *par-2* mutant embryos, P_1 rotation does not take place and PAR-3 is distributed evenly around the cortex of the P_1 blastomere, as in *ooc-3* mutant embryos. Since rotation can be induced in *par-2;par-3* double mutant embryos, it is thought that the even distribution of PAR-3 throughout the cortex prevents P_1 rotation (Cheng et al., 1995). We wanted to investigate whether the defect in P_1 rotation in *ooc*-3 mutant embryos was also due to even distribution of PAR-3 on the cortex of the P_1 blastomere. To address this question we silenced *par-3* expression in *ooc-3* mutant embryos by RNAi and scored rotation of the centrosome-nucleus complex in both AB and P_1. We used the *mn241* allele, which has the most penetrant defect in PAR-3 localization. Silencing of *par-3* expression in the *ooc-3(mn241)* background gave rise to embryos in which first cleavages were symmetric and second cleavages were synchronous, suggesting that both blastomeres had similar identity. P_1 rotation in the *mn241* single mutant was successful only in 10% of the embryos (Table 2). In contrast, silencing of *par-3* expression in the *ooc-3* (*mn241*) mutant background lead to rotation in 40% of P_1-like blastomeres and 65% of AB-like blastomeres (Table 2). Therefore we conclude that the defect in P_1 rotation in *ooc-3* mutant embryos is due, at least in part, to even distribution of PAR-3 on the cortex of the P_1 blastomere

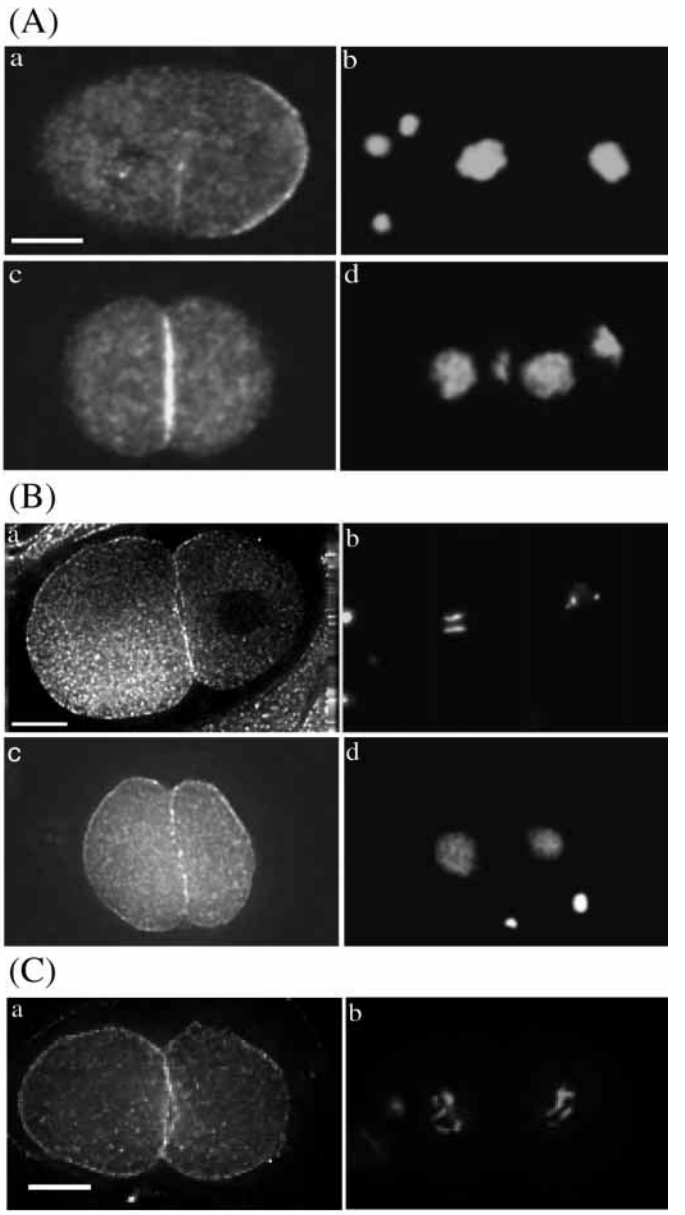

Fig. 6. *ooc-3* is required for the localization of PAR-2 and PAR-3 to the anterior and posterior cortices, respectively. Wild-type and *ooc-3* mutant embryos were stained with anti-PAR-2 (A), anti-PAR-3 (B) and *ooc-3;par-3* double mutants were stained with PAR-2 antibody (C) and counterstained with Hoechst 33258 to reveal DNA. Images are 2 μm confocal slices Anterior is to the left. (A) PAR-2 staining of wild-type and *ooc-3* mutant embryos. (a,b) Wild-type PAR-2 is localized at the posterior cortex of P_1. Traces of PAR-2 can be detected at the anterior cortex of P_1. P_1 is in prophase. (a) PAR-2, (b) DNA. (c,d) In an *ooc-3* mutant PAR-2 is localized at the anterior cortex of P_1. P_1 is in prophase. (c) PAR-2, (d) DNA. (B) PAR-3 staining of wild-type and *ooc-3* mutant embryos. (a,b) Wild-type PAR-3 is localized at the anterior cortex of P_1. P_1 is in prophase. (a) PAR-3, (b) DNA. (c,d) *ooc-3* mutant PAR-3 is localized all around the cortex of P_1. P_1 is in prophase. (c) PAR-3, (d) DNA. (C) PAR-2 staining of *ooc-3* mutants lacking *par-3* function. PAR-2 is localized all around the cortex in P_1. P_1 is in prophase. (a) PAR-2, (b) DNA. Bar, 10 μm.

Table 2. Silencing of PAR-3 expression in *ooc-3* mutant embryos induces rotation of the centrosome-nucleus complex

Genotype	No. of embryos	% both spindles longitudinal AB ↔ ↔ P_1	% both spindles transverse AB ↕ ↕ P_1	% wild type AB ↕ ↔ P_1	% inverse AB ↔ ↕ P_1
par-3(RNAi)	8	88	0	0	12
ooc-3(mn241)	10	0	90[1]	10	0
ooc-3(mn241); par-3(RNAi)	20	15[2]	10	25	50[3]

PAR-3 expression was silenced in wild-type and *ooc-3* mutant embryos by RNA interference (RNAi). Rotation of the centrosome-nucleus complex was scored 24 hours postinjection in *par-3(RNAi)*, *ooc-3(mn241)* and *ooc-3(mn241), par-3 (RNAi)* embryos using the 'hanging-drop' method (see Materials and Methods).
[1]In 2/9 embryos the P_1 spindle and in 4/9 embryos the AB spindle rotates 90°.
[2]The P_1 spindle rotates 90° in 2/3 embryos.
[3]In 5/10 embryos the AB spindle rotates 90°.

OOC-3 is a novel transmembrane protein

To determine the molecular nature of *ooc-3*, we cloned the gene by cosmid rescue using germline transformation (Fig. 7A). Rescue of the maternal-effect lethality with an approx. 3.2 kb genomic fragment revealed that *ooc-3* is encoded by the B0334.11 gene (see Materials and Methods). Silencing of that gene by RNAi inhibited P_1 rotation in 100% of embryos examined 22-24 hours post injection (see Materials and Methods). OOC-3 is predicted to encode a 448 amino acid (aa), 51 kDa protein with an isoelectric point (pI) of 5.13. OOC-3 has no significant homology to any known proteins. Sequence analysis suggested the following structural features for the OOC-3 protein: a signal peptide from aa 1-17 and three transmembrane domains from aa 150-166, 175-191 and 294-310, respectively (Fig. 7B). Thus, OOC-3 is a putative transmembrane protein. Sequence prediction suggests a putative membrane topology in which the C-terminus is cytosolic and the N-terminus luminal. Furthermore, OOC-3 contains two putative PEST sequences at its carboxy terminus (from aa 400 to 430), common to rapidly degraded proteins (Rogers et al., 1986). In order to identify the parts of the OOC-3 protein that play an essential role in its function we sequenced the *mn241* and the *t1308* alleles. This revealed a STOP codon at nucleotide position 777 right after the second transmembrane domain in *t1308* and a mutation at position 886 in the 3′ splice site before the third transmembrane domain for *mn241* (see Materials and Methods). Thus, the predicted cytoplasmic tail, which is missing in both alleles that were sequenced, is essential for *ooc-3* function.

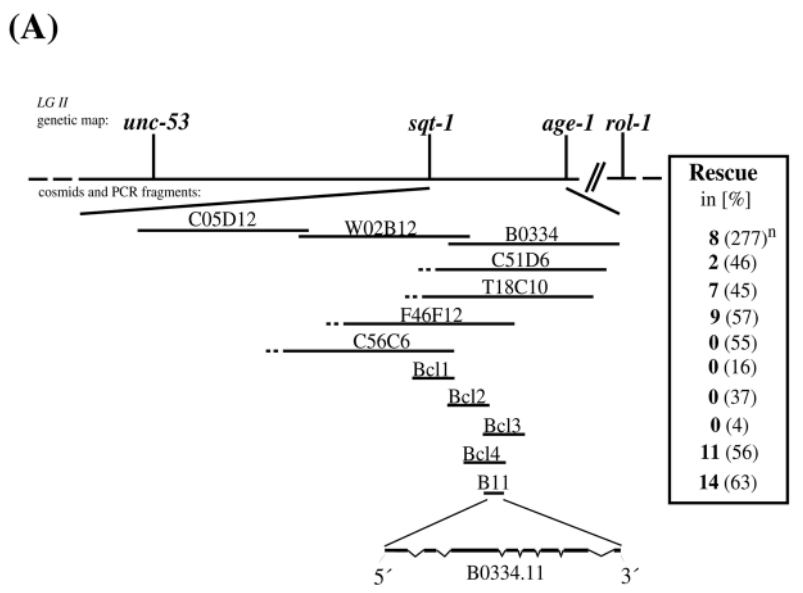

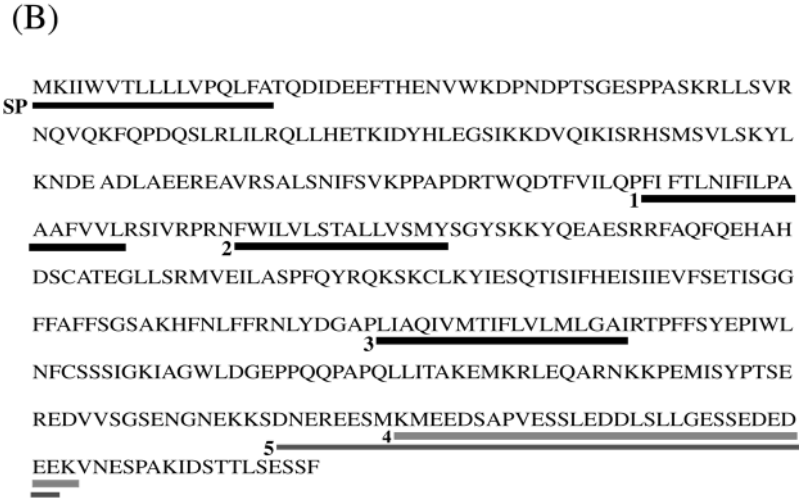

OOC-3 probably localizes to the endoplasmic reticulum and its distribution is dynamic in the early embryo

To investigate the localization of OOC-3 we raised a polyclonal C-terminal anti-peptide antibody

Fig. 7. Cloning of *ooc-3: ooc-3* encodes a novel putative transmembrane protein. (A) Genetic mapping put *ooc-3* between *unc-53* and *age-1*. The cosmids B0334, C51D6, T18C10 and F46F12 and the PCR fragments Bcl4 and B11 rescued the maternal-effect lethality using a germline transformation assay (see Materials and Methods). *n*, number of worms analysed. (B) The OOC-3 protein sequence. The black underlined region (SP) represents a signal peptide sequence (1-17), the three other black underlined regions (1,2 and 3) represent putative transmembrane domains (149-166, 175-189 and 293-310). The grey underlined region (4) represents a negatively charged cluster (392-429), and the grey open-box underlined region (5) two putative PEST sequences (400-430).

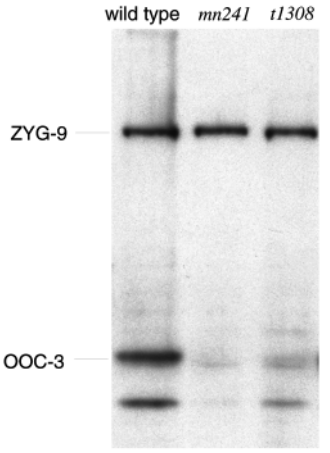

Fig. 8. Western blot analysis of OOC-3 protein. Western blot analysis was performed with mixed staged wild-type and *ooc-3* mutant embryos (*t1308*, *mn241*). OOC3Ct2 recognizes a band of 51 kDa, which is essentially absent in *ooc-3* mutant embryos. The lower band is probably a degradation product. Antibodies against ZYG-9 were used as a loading control.

(OOC3Ct2) against a peptide spanning aa 432-448 (see Materials and Methods). OOC3Ct2 recognized a band of about 50 kDa by western blotting, similar to the predicted molecular mass of 51.5 kDa. No protein was detected in extracts of *t1308* in which the C-terminus is missing and almost no protein was present in extracts of *mn241* mutant worms in which *ooc-3* is mis-spliced (Fig. 8).

We analyzed the subcellular distribution of OOC-3 using the OOC3Ct2 antibody. Overall, OOC-3 is localized to a membrane compartment that had a dynamic distribution through the cell cycle. From fertilization until the beginning of pronuclear migration OOC-3 is uniformly enriched at the cortex of P_0 in 75% of the embryos (n=36) (Fig. 9a). At the beginning of pronuclear migration the cortical staining diminishes and OOC-3 is enriched around pronuclei (n=10) (data not shown). During rotation in P_0, OOC-3 redistributes to the asters (Fig. 9c) and in mitosis OOC-3 becomes enriched at the mitotic spindle (Fig. 9e). Towards the beginning of prophase of two-cell stage embryos OOC-3 localizes to a reticular structure spanning the whole cytoplasm, being enriched at the circumference of nuclei (Fig. 10a). In mitosis it again localizes to the mitotic spindle (Fig. 10c). The reticular localization can be more clearly seen in a threefold enlargement taken using a deconvolution microscope (Fig. 10g). The distribution of OOC-3 is reminiscent of the endoplasmic reticulum (ER) in other species (Henson et al., 1989; Terasaki and Jaffe, 1991). We confirmed the ER localization by staining *C. elegans* embryos with an antibody to HDEL (data not shown), a sequence responsible for retention of proteins in the ER. OOC-3 is slightly enriched at the cell-cell boundary between AB and P_1 in 50% of the embryos examined (n=45) (black arrowheads, Fig. 10a) and more strongly at cell-cell boundaries (black arrowhead, Fig. 10e) of 100% of the four-cell stage embryos examined (n=28). We observed no specific staining in *ooc-3 (t1308)* mutant embryos using the OOC3Ct2 antibody (Fig. 9g), and peptide competition prevented specific staining (Fig. 9i), demonstrating that OOC3Ct2 is an antibody specifically recognizing OOC-3 protein.

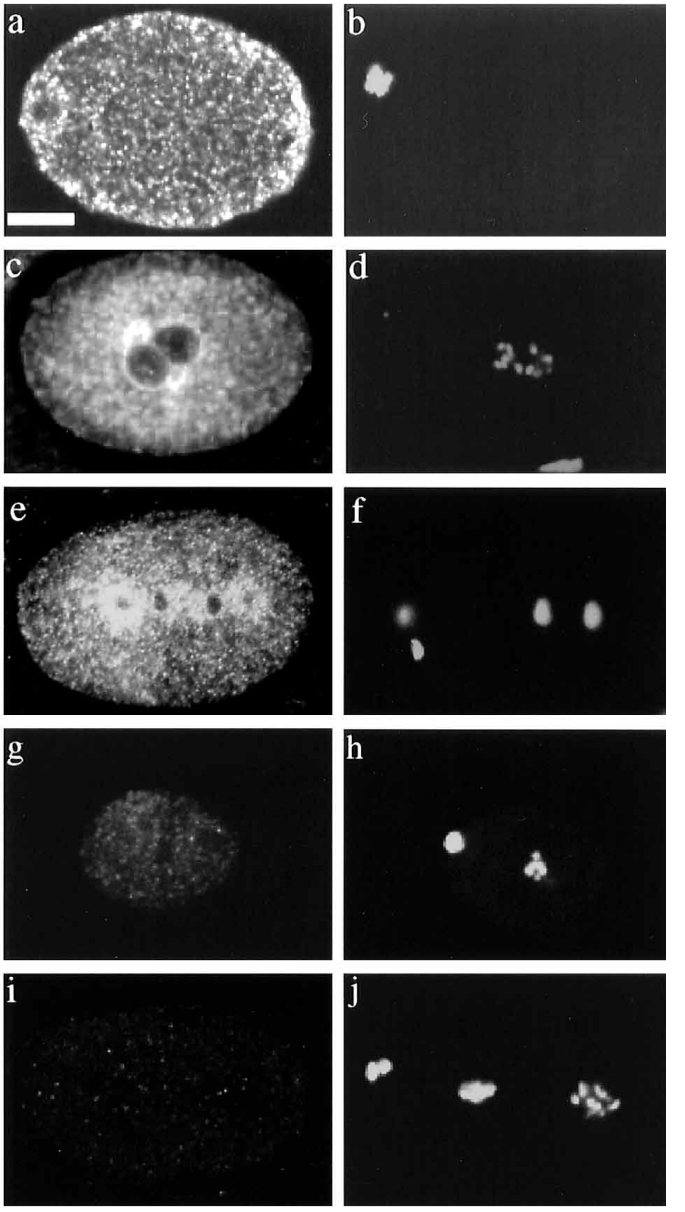

Fig. 9. OOC-3 localization in one-cell stage embryos. Confocal micrographs of embryos that have been stained with OOC3Ct2 to reveal the localization of OOC-3 protein and counterstained with Hoechst 33258 to reveal the DNA. (a,b) One-cell stage embryos at fertilization. OOC-3 localizes under the cortex of the embryo. (a) OOC-3, (b) DNA. (c,d) One-cell stage embryo at P_0 rotation. OOC-3 localizes to a reticular structure spanning the whole cytoplasm being enriched at the circumference of nuclei and the asters. (c) OOC-3, (d) DNA. (e,f) One-cell stage embryo in mitosis. OOC-3 localizes to the mitotic spindle. (e) OOC-3, (f) DNA. (g,h) *ooc-3* mutant embryo at the time of P_1 rotation. Staining with antibody to OOC-3. No staining reminiscent of OOC-3 could be observed. (g) OOC-3, (h) DNA. (i,j) Peptide competition. Wild-type embryo at pronuclear migration stained with a mixture of OOC3Ct2 and the peptide against OOC3Ct2. No staining reminiscent of OOC-3 could be observed. (i) OOC-3, (j) DNA. Bar, 10 μm.

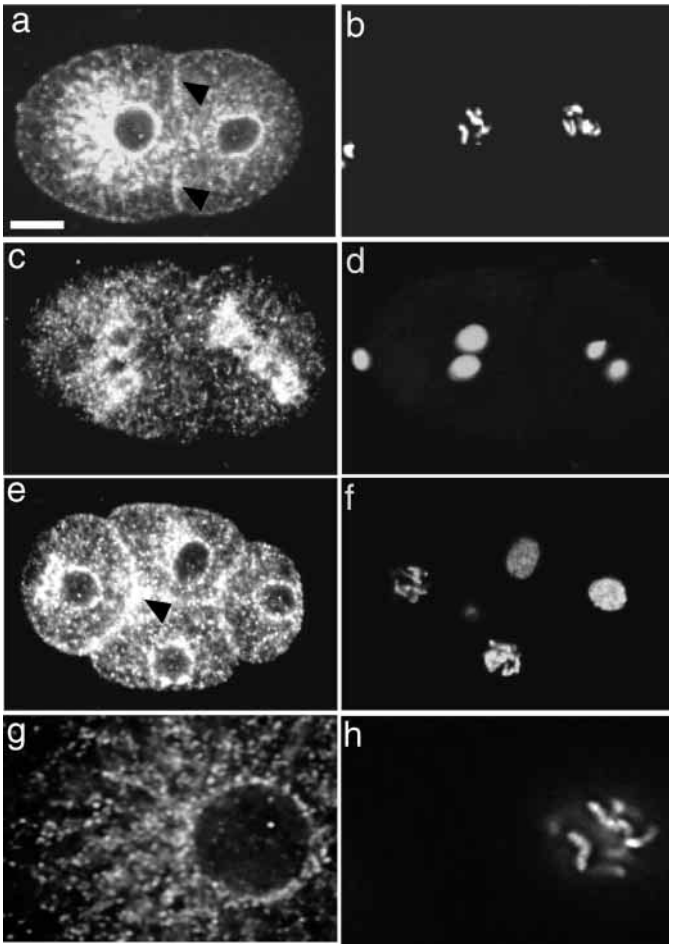

Fig. 10. OOC-3 localization in two- and four-cell stage embryos. Confocal micrographs of embryos that have been stained with OOC3Ct2 to reveal the localization of OOC-3 protein and counterstained with Hoechst 33258 to reveal DNA. (a,b) Prophase of two-cell stage embryo. OOC-3 localizes to a reticular structure spanning the whole cytoplasm being enriched at the perinuclear region. Furthermore, it is slightly enriched at the cell-cell boundary (black arrowheads). (a) OOC-3, (b) DNA. (c,d) In mitosis OOC-3 localizes to the mitotic spindle. (c) OOC-3, (d) DNA. (e,f) In four-cell stage embryos OOC-3 localizes to the circumference of nuclei and to a reticular structure spanning the cytoplasm. Furthermore, the protein is enriched at the cell-cell boundaries (black arrowhead). (e) OOC-3, (f) DNA. (g,h) 0.2 μm slice taken with a Deltavision microscope and deconvolved. Enlargement to show the reticular structure and outline of the nuclear envelope of OOC-3 in a prophase cell. (g) OOC-3, (h) DNA. Bar, 10 μm.

DISCUSSION

OOC-3 is required for the orientation of the mitotic spindle in P_1 blastomeres

One of the most striking phenotypes of *ooc-3* mutants is the failure to correctly align the division axis at the two-cell stage. In the P_1 blastomere of wild-type embryos, orientation of the mitotic spindle along the antero-posterior axis depends on a 90° rotation of the centrosome-nucleus complex (Hyman and White, 1987; Hyman, 1989). Not much it known about this process, but it is thought to occur by capture of the microtubules emanating from one centrosome by a cortical site at the anterior cortex (Hyman, 1989; Strome and White, 1996).

Why does rotation fail in *ooc-3* mutant embryos? One of the markers of the cortical site is a ring of actin on the anterior cortex of P_1 (Waddle et al., 1994; Skop and White, 1998). Our examination of the distribution of actin on the anterior cortex of P_1 suggests that the structure of the cortical site itself may be disturbed. While we cannot say for sure that rotation fails because of a change in the cortical site, it is interesting that the centrosomes in *ooc-3* mutants are positioned around the nucleus closer to the anterior cortex. This raises the possibility that force is being exerted on both centrosomes rather than just one, as in wild type. The mechanism by which force generation during rotation in wild type is limited to one centrosome only is unknown. One possibility is that it depends on restricting the size of the cortical site. According to this model rotation in *ooc-3* mutants would fail because an enlarged cortical site captures many microtubules from both centrosomes. Thus pulling forces, instead of exerting torque on the centrosome-nucleus complex to execute rotation, would pull the centrosome-nucleus complex towards the anterior cortex, eventually pulling both centrosomes around the nuclear envelope. A similar phenotype, in which centrosomes move around the nuclear envelope towards the anterior cortex, can sometimes be seen in wild-type embryos when rotation fails (see Hyman, 1989, Fig. 7).

OOC-3 is required for the correct localization of PAR-2 and PAR-3 at the two-cell stage

Why are rotation and the organization of the cortical site defective in OOC-3 mutants? The fact that downstream events of embryonic polarity such as P-granule segregation and P_1 rotation fail suggests a general defect in polarity. In the P_1 blastomere, establishment of the antero-posterior axis depends upon the localization of PAR-2 to the posterior cortex and PAR-3 to the anterior cortex, forming two cortical domains (Rose and Kemphues, 1998). Our analysis has shown that the localization of the PAR proteins is defective in *ooc-3* mutants: PAR-3 is evenly distributed on the cortex and PAR-2 is confined to the anterior cortex, so that on the anterior cortex, PAR-2 and PAR-3 overlap. Thus in *ooc-3* mutants, these mutually exclusive cortical domains fail to form.

Therefore it is possible that rotation fails in *ooc-3* mutants because of defects in cell polarity. However we know that *ooc-3* is required to organize the cortical actin cytoskeleton at the cell-cell boundary. Furthermore, it is known that the actin cytoskeleton is required for correct polarity and rotation (Hill and Strome, 1988, 1990). Therefore, we do not know whether in *ooc-3* mutants, this disruption of cortical actin staining is due to mislocalization of the PAR proteins, or whether *ooc-3* mutants cause misorganization of the actin cytoskeleton, preventing correct PAR localization, or whether the two processes are independent of each other.

Some insight into this issue has come from our analysis of whether rotation of the centrosome-nucleus complex in P_1 fails because of the symmetric localization of PAR-3. Silencing of *par-3* expression in *ooc-3* mutant embryos allowed rotation to occur in at least one blastomere in most embryos lacking *ooc-3* and *par-3* function. This clearly demonstrates that rotation partially fails in *ooc-3* mutants because of the symmetric distribution of PAR-3, but that this is not the only factor. This

result could be explained if OOC-3 acts in part independently of PAR-3, perhaps through the actin cytoskeleton, to organize the anterior cortex of the P_1 blastomere.

Establishment of cortical domains is mediated through *ooc-3*

Our data have implications for the mechanisms of PAR localization. Previous studies of the localization of the PAR proteins have suggested that PAR-2 and PAR-3 mutually exclude each other from the cortex (Etemad-Moghadam et al., 1995). These studies have not addressed whether PAR-2 or PAR-3 is the primary cue for establishing cortical domains. Does PAR-2 localize first and then exclude PAR-3, or does PAR-3 localize first and exclude PAR-2? Our results suggest that at least in the two-cell stage, mislocalization of PAR-3 in *ooc-3* mutants confines PAR-2 to the anterior cortex. If PAR-3 is removed in an *ooc-3* mutant, PAR-2 is now free to localize around the cortex. These results suggest a model in which, following the first cell division in wild type, OOC-3 is required to create a cortical domain of PAR-3 on the anterior cortex. This in turn excludes PAR-2 from the anterior cortex.

How could OOC-3 restrict PAR-3 to the anterior cortex? The bulk of OOC-3 protein localizes to a membrane compartment that resembles the endoplasmic reticulum in other organisms (Henson et al., 1989; Terasaki and Jaffe, 1991; Ioshii et al., 1995) and is similar to the distribution of proteins carrying the HDEL sequence. One possibility is that OOC-3 is an ER resident protein with an ER function. Trafficking of proteins required for correct polarity may be thus affected in *ooc-3* mutant embryos. The OOC-3 protein, however, does not contain any known sorting signals that restrict localization of proteins to the ER (Nilsson et al., 1989; Schutze et al., 1994; Munro and Pelham, 1987). Another possibility is that OOC-3 would direct proteins required for polarity by accompanying them to the correct place in the cell. This model would be consistent with the emerging paradigm for proteins that localize to the ER and are involved in targeting polarity proteins to the correct place in the cell. In *S. cerevisiae*, Axl2, a protein required for bud site selection and subsequent establishment of polarity is delivered to nascent bud tips via Erv14, an ER-vesicle protein. In erv-14 mutants, Axl2 accumulates in the ER and axial budding pattern is disturbed (Powers and Barlowe, 1998). In *C. elegans* embryos, members of the p24 family of proteins, which have been implicated in cargo selectivity of ER to Golgi transport, are involved in trafficking of LIN-12 and GLP-1, proteins required for mediating cell-cell interactions during the specification of cell fate (Levitan and Greenwald, 1998). Therefore it is clear that specific targeting of transmembrane proteins during their passage through the ER is important for the establishment of polarity.

A distinct mechanism for establishing polarity following cell division

Our analysis shows that *ooc-3* is required for establishment of cortical domains in P_1 and not in P_0. We have noted that the late anaphase spindle in P_0 of *ooc-3* mutant embryos is located more to the cell center than in wild type, resembling the spindle position observed in *par* mutant embryos. However, in contrast to *par* mutant embryos, the first division is not fully symmetric, and the divisions of AB and P_1 are not synchronous in *ooc-3* mutant embryos. Moreover, the segregation of P granules and the expression of PAR-2 protein is never altered in P_0, while that of PAR-3 is altered in a minority of embryos in a single allele. Taken together, these observations suggest that *ooc-3* is largely dispensable for establishment of cortical domains in P_0, but may be required for communication between the polarity and the cytoskeleton in that cell.

In contrast, the data presented in this paper clearly demonstrate that *ooc-3* is required for the establishment of cortical domains in P_1. Why would *ooc-3* be differentially required for establishment of polarity in P_0 and in P_1? In P_0, the establishment of the antero-posterior axis, and therefore localization of the PAR proteins, is mediated by the entry of the sperm and this appears to be an *ooc-3*-independent process. However, polarity must be re-established after each cell division, and this mechanism cannot involve the sperm entry point. We do not know what the polarity cues are following cell division, but cell-cell boundaries have been suggested to serve as intrinsic cues for the establishment and maintenance of cortical domains in epithelial cells (Böhm et al., 1997). In axial budding of *S. cerevisiae*, the cell division remnant serves as an initial asymmetric cue for the recruitment of the bud-site selection and polarity-establishment proteins. Since a subset of the OOC-3 protein is localized at the cell-cell boundary in two-cell stage embryos, one could imagine that in *C. elegans* the cell-cell boundary serves as the intrinsic cue. A caveat is that isolated P_1 blastomeres appear to be able to polarize on their own (Goldstein, 1993); however, the blastomeres cannot be separated until the division is complete and the two cells are no longer connected, by which time polarity may be established.

The authors thank Ken Kemphues, Bruce Bowerman and James Waddle for generous gifts of antibodies, Arshad Desai, Suzanne Eaton, Chris Echeverri, Leslie Rose and Kai Simons for helpful discussions and critical reading of the manuscript and Sean Munroe for antibodies to HDEL and helpful conversations.

REFERENCES

Albertson, D. (1984). Formation of the first cleavage spindle in nematode embryos. *Dev. Biol.* **101**, 61-72.

Böhm, H., Brinkmannj, V., Drab, M., Henske, A. and Kurzchalia, T. (1997). Mammalian homologues of *C. elegans* PAR-1 are asymmetrically localized in epithelial cells and may influence their polarity. *Curr. Biol.* **7**, R603-R606.

Boyd, L., Guo, S., Levitan, D., Stinchcomb, D. T. and Kemphues, K. J. (1996). PAR-2 is asymmetrically distributed and promotes association of P granules and PAR-1 with the cortex in *C. elegans* embryos. *Development* **122**, 3075-3084.

Brenner, S. (1974). The genetics of *Caenorhabditis elegans*. *Genetics* **77**, 71-94.

Chant, J. and Pringle, J. R. (1991). Budding and cell polarity in *Saccharomyces cerevisiae*. *Curr. Opin. Genet. Dev.* **1**, 342-350.

Cheng, N. N., Kirby, C. M. and Kemphues, K. J. (1995). Control of cleavage spindle orientation in *Caenorhabditis elegans*: the role of the genes *par-2* and par-3. *Genetics* **139**, 549-559.

Drubin, D. G. and Nelson, W. J. (1996). Origins of cell polarity. *Cell* **84**, 335-344.

Etemad-Moghadam, B., Guo, S. and Kemphues, K. J. (1995). Asymmetrically distributed PAR-3 protein contributes to cell polarity and spindle alignement in early *C. elegans* embryos. *Cell* **83**, 743-752.

Fire, A., Xu, S., Montgomery, M. K., Kostas, S. A., Driver, S. E. and Mello, C. C. (1998). Potent and specific genetic interference by double-stranded RNA in *Caenorhabditis elegans*. *Nature* **391**, 806-811.

Goldstein, B. (1993). Establishment of gut fate in the E lineage of *C. elegans*:

the roles of lineage-dependent mechanisms and cell interactions. *Development* **118**, 1267-1277.

Goldstein, B. and Hird, S. N. (1996). Specification of the anteroposterior axis in *Caenorhabditis elegans*. *Development* **122**, 1467-1474.

Gönczy, P. and Hyman, A. A. (1996). Cortical domains and the mechanisms of asymmetric cell division. *Trends Cell Biol.* **6**, 382-387.

Gönczy, P., Schnabel, H., Kaletta, T., Amores, A. D., Hyman, T. and Schnabel, R. (1999). Dissection of cell division processes in the one cell stage *Caenorhabditis elegans* embryo by mutational analysis. *J. Cell Biol.* **144**, 927-946.

Guo, S. and Kemphues, K. J. (1995). par-1, a gene required for establishing polarity in *C. elegans* embryos, encodes a putative Ser/Thr kinase that is asymmetrically distributed. *Cell* **81**, 611-620.

Henson, J. H., Begg, D. A., Beaulieu, S. M., Fishkind, D. J., Bonder, E. M., Terasaki, M., Lebeche, D. and Kaminer, B. (1989). A calsequestrin-like protein in the endoplasmic reticulum of the sea urchin: localization and dynamics in the egg and first cell cycle embryo. *J. Cell Biol.* **109**, 149-61.

Herman, R. K. (1978). Crossover suppressors and balanced recessive lethals in *C. elegans. Genetics* **149**, 1303-1321.

Hill, D. P. and Strome, S. (1988). An analysis of the role of microfilaments in the establishment and maintenance of asymmetry in *Caenorhabditis elegans* zygotes. *Dev. Biol.* **125**, 75-84.

Hill, D. P. and Strome, S. (1990). Brief cytochalasin-induced disruption of microfilaments during a critical interval in 1-cell *C. elegans* embryos alters the partitioning of developmental instructions to the 2-cell embryo. *Development* **108**, 159-172.

Horvitz, H. R. and Herskowitz, I. (1992). Mechanisms of asymmetric cell division: two Bs or not two Bs, that is the question. *Cell* **68**, 237-255.

Hyman, A. A. (1989). Centrosome movement in the early divisions of *Caenorhabditis elegans*: a cortical site determining centrosome position. *J. Cell Biol.* **109**, 1185-1193.

Hyman, A. A. and White, J. G. (1987). Determination of cell division axes in the early embryogenesis of *Caenorhabditis elegans*. *J. Cell Biol.* **105**, 2123-2135.

Ioshii, S. O., Yoshida, T., Imanaka-Yoshida, K. and Izutsu, K. (1995). Distribution of a Ca^{2+} storing site in PtK2 cells during interphase and mitosis. An immunocytochemical study using an antibody against calreticulin. *Eur. J. Cell Biol.* **66**, 82-93.

Kemphues, K. J., Kusch, M. and Wolf, N. (1988). Maternal-effect lethal mutations on linkage group II of *Caenorhabditis elegans*. *Genetics* **120**, 977-986.

Kuchinke, U., Grawe, F. and Knust, E. (1998). Control of spindle orientation in *Drosophila* by the Par-3-related PDZ- domain protein Bazooka. *Curr. Biol.* **8**, 1357-1365.

Levitan, D. and Greenwald, I. (1998). Effects of SEL-12 presenilin on LIN-12 localization and function in *Caenorhabditis elegans*. *Development* **125**, 3599-3606.

Levitan, D. J., Boyd, L., Mello, C. C., Kemphues, K. J. and Stinchcomb, D. T. (1994). *par-2*, a gene required for blastomere asymmetry in *Caenorhabditis elegans*, encodes zinc-finger and ATP-binding motifs. *Proc. Natl. Acad. Sci. USA* **91**, 6108-6112.

Madden, K. and Snyder, M. (1998). Cell polarity and morphogenesis in budding yeast. *Annu. Rev. Microbiol.* **52**, 687-744.

Matthews, L. R., Carter, P., Thierry, M. D. and Kemphues, K. (1998). ZYG-9, a *Caenorhabditis elegans* protein required for microtubule organization and function, is a component of meiotic and mitotic spindle poles. *J. Cell Biol.* **141**, 1159-1168.

Mello, C. C., Kramer, J. M., Stinchcomb, D. and Ambros, V. (1991). Efficient gene transfer in *Caenorhabditis elegans*: extrachromosomal maintenance and integration of transforming sequences. *EMBO J.* ***10,***, 3959-3970.

Munro, S. and Pelham, H. R. (1987). A C-terminal signal prevents secretion of luminal ER proteins. *Cell* **48**, 899-907.

Nilsson, T., Jackson, M. and Peterson, P. A. (1989). Short cytoplasmic sequences serve as retention signals for transmembrane proteins in the endoplasmic reticulum. *Cell* **58**, 707-718.

O'Connell, K. F., Leys, C. M. and White, J. G. (1998). A genetic screen for temperature-sensitive cell-division mutants of *Caenorhabditis elegans. Genetics* **149**, 1303-1321.

Pearson, W. R. and Lipman, D. J. (1988). Improved tools for biological sequence comparison. *Proc. Natl. Acad. Sci. USA* **85**, 2444-2448.

Powers, J. and Barlowe, C. (1998). Transport of Axl2p depends on Erv14p, an ER-vesicle protein related to the *Drosophila cornichon* gene product. *J. Cell Biol.* **142**, 1209-1222.

Rogers, S., Wells, R. and Rechsteiner, M. (1986). Amino acid sequences common to rapidly degraded proteins: the PEST hypothesis. *Science* **234**, 364-368.

Rose, L. S. and Kemphues, K. J. (1998). Early patterning of the *C. elegans* embryo. *Annu. Rev. Genet.* **32**, 521-545.

Roth, S., Neuman-Silberberg, F. S., Barcelo, G. and Schupbach, T. (1995). Cornichon and the EGF receptor signaling process are necessary for both anterior-posterior and dorsal-ventral pattern formation in *Drosophila*. *Cell* **81**, 967-978.

Schutze, M. P., Peterson, P. A. and Jackson, M. R. (1994). An N-terminal double-arginine motif maintains type II membrane proteins in the endoplasmic reticulum. *EMBO J.* **13**, 1696-1705.

Sigurdson, D. C., Spanier, G. J. and Herman, R. K. (1984). *Caenorhabditis elegans* deficiency mapping. *Genetics* **108**, 331-345.

Skop, A. R. and White, J. G. (1998). The dynactin complex is required for cleavage plane specification in early *Caenorhabditis elegans* embryos. *Curr. Biol.* **8**, 1110-1115.

Strome, S. and White, J. (1996). Cleavage Plane Specification. *Cell* **84**, 195-198.

Strome, S. and Wood, W. B. (1983). Generation of asymmetry and segregation of germ-line granules in early *C. elegans* embryos. *Cell* **35**, 15-25.

Tabuse, Y., Izumi, Y., Piano, F., Kemphues, K. J., Miwa, J. and Ohno, S. (1998). Atypical protein kinase C cooperates with PAR-3 to establish embryonic polarity in *Caenorhabditis elegans*. *Development* **125**, 3607-3614.

Terasaki, M. and Jaffe, L. A. (1991). Organization of the sea urchin egg endoplasmic reticulum and its reorganization at fertilization. *J. Cell Biol.* **114**, 929-940.

Waddle, J. A., Cooper, J. A. and Waterston, R. H. (1994). Transient localized accumulation of actin in *Caenorhabditis elegans* blastomeres with oriented asymmetric divisions. *Development* **120**, 2317-2328.

Watts, J. L., Etemad-Moghadam, B., Guo, S., Boyd, L., Draper, B. W., Mello, C. C., Priess, J. R. and Kemphues, K. J. (1996). *par-6*, a gene involved in the establishment of asymmetry in early *C. elegans* embryos, mediates the asymmetric localization of PAR-3. *Development* **122**, 3133-3140.